

NUMERICAL SIMULATION OF MIXED-MODE FRACTURE IN CONCRETE VIA A NON-LOCAL DAMAGE MODEL

Liberato Ferrara¹

*Politecnico di Milano, Department of Structural Engineering
piazza Leonardo da Vinci 32, 20133 Milano, Italy*

SUMMARY

A "slightly" modified version of the "crush-crack" damage model (di Prisco and Mazars, 1996) is here presented and applied to numerical analysis of typical mixed-mode fracture tests. Besides the validation of the proposed modifications, the work is also instrumental in understanding the reliability of either the shear behaviour description supplied by the model and of the proposed test geometries as tools for identifying mixed-mode fracture parameters.

Keywords: mixed-mode fracture, damage mechanics, non-local models.

1. INTRODUCTION

Despite crack initiation, in both plain and reinforced concrete structures, occurs in mode I, i. e. at a right angle to the maximum principal stress, coupling of either opening and sliding fracture modes (mixed mode I+II) may likewise take place, owing to the boundary conditions, to the interaction with reinforcing bars as well as to the roughness of crack surfaces. The slight activation of a sliding mode may even feature the so-called "uniaxial tensile tests", due to a combined action of boundary restraints and tortuosity of crack paths, thus giving rise to a global energy dissipation bigger than mode I fracture energy, G_{If} , and, moreover, contributing to cast some doubts over the reliability of such a tests in order to identify mode I fracture parameters (see, e.g., van Mier, 1997). A suitable description of concrete behaviour under mixed-mode loadings as well as a careful identification of mixed-mode fracture parameters are therefore of utmost importance if one wants to formulate reliable models for predictive analysis of plain and r/c structures. The problem is furthermore complicated as the same existence of mode II fracture in concrete, as well as the consequent definition of a mode II fracture energy, G_{IIIf} , are still widely open and highly debated questions (see Ferrara, 1998, for a review). Several test geometries have been proposed over the past few decades, with the aim of studying crack growth under combined tensile and shear loads and of extracting information to extend to shear non-linear fracture models, originally formulated in the context of a pure mode I fracture.

In this work the Four Edged Notched (FEN) box tested by Hassanzadeh (1991) and the Double Edge Notched (DEN) plate tested by Nooru-Mohammed (1992), have been analyzed, with reference to some among the several load-paths experimentally performed; the numerical simulations have been carried out adopting a modified version of the "Crush-Crack" damage model (di Prisco and Mazars, 1996). After the

¹ PhD student

presentation of the model, the investigation on mixed-mode fracture will be addressed, first with reference to some simple model problems, in order to check the reliability of the proposed modified version of the model itself. Thereafter, the above said experimental tests will be numerically analyzed. The twofold purpose of the work is to carry on the investigation on predictive capabilities of the model (see also di Prisco et al., 1998), which does not provide an explicit description for shear but simply regards it as a biaxial tension-compression stress state, and to assess the reliability of the proposed test geometries as tools for the identification of mixed-mode fracture parameters.

2. MODEL FORMULATION AND MIXED-MODE VERIFICATION

"Crush-Crack" non-local damage model (di Prisco and Mazars, 1996) couples elastic stiffness degradation with cumulation of both tensile and compressive irreversible strains, thus aiming at a description of either cracking and crushing phenomena, which feature concrete behaviour and are responsible of its nonlinearity. Furthermore, the introduction of a second internal variable δ , besides the damage one D , allows to capture, through the evolution of Poisson's ratio, reversible dilation phenomena. It carries too far to give in this paper a detailed analytical formulation of the model; the reader is referred to the above quoted reference. It is nevertheless worth remarking that, though the key idea of a unique scalar damage variable is still preserved, its evolution is split into three different contributions associated to the three basic failure modes observed for concrete, respectively uniaxial tension, biaxial compression and uniaxial compression (van Mier, 1997)- let us say D_t , D_c^I and D_c^{II} - whose evolution is governed by a non-local strain invariant $\bar{\epsilon}$. Such a quantity is calculated averaging a local strain invariant, built with the positive parts of the elastic and irreversible strains, over a support whose diameter is set equal to $3l$, where l is an internal length, related to the material characteristic length or to the crack band width, as shown, e.g., in (di Prisco and Ferrara, 1996). The compressive damage components are combined, by means of a suitable function, into a unique "indirect damage" contribution D_c , which is further combined with the "direct" (tensile) damage contribution, so to obtain the scalar damage variable D :

$$D = \alpha_c D_c + \alpha_t D_t \quad (1)$$

In the original model formulation, weighting functions α_c and α_t are calculated as:

$$\alpha_c = \frac{\sum_{i=1}^3 \frac{\epsilon_{ci}^{el} (\epsilon_{ti}^{el} + \epsilon_{ci}^{el})}{\sum_{i=1}^3 (\epsilon_{ti}^{el} + \epsilon_{ci}^{el})^2}}{\sum_{i=1}^3 \frac{\epsilon_{ti}^{el} (\epsilon_{ti}^{el} + \epsilon_{ci}^{el})}{\sum_{i=1}^3 (\epsilon_{ti}^{el} + \epsilon_{ci}^{el})^2}} \quad \alpha_t = \frac{\sum_{i=1}^3 \frac{\epsilon_{ti}^{el} (\epsilon_{ti}^{el} + \epsilon_{ci}^{el})}{\sum_{i=1}^3 (\epsilon_{ti}^{el} + \epsilon_{ci}^{el})^2}}{\sum_{i=1}^3 \frac{\epsilon_{ti}^{el} (\epsilon_{ti}^{el} + \epsilon_{ci}^{el})}{\sum_{i=1}^3 (\epsilon_{ti}^{el} + \epsilon_{ci}^{el})^2}} \quad (2)$$

where ϵ_{ti}^{el} and ϵ_{ci}^{el} are the positive parts of the elastic strain respectively associated to tensile and compressive stresses.

The response of the model, in its original formulation, has been checked with reference to some simple mixed-mode homogeneous tests: a CST finite element, in plane strain conditions (see Fig.1a) is first subjected to uniaxial tension up to the peak and, subsequently, to normal and tangential displacements, simultaneously applied according to the following relationship:

$$\delta_s = \delta_n \operatorname{tg} \alpha \quad (3)$$

with α , equal to 30° , 45° , 60° and 75° . The above said load paths coincide with those experimentally tested by Hassanzadeh (1991). His experimental setup being such that an

almost uniform process zone subjected to mixed-mode loading was created inside the Four Edge Notched (FEN) specimen, the tests have been regarded by several authors as suitable for the so-called "mixed-mode constitutive verification" of a model, even within different crack methodologies (Carol et al., 1997; Ohlsson and Olofsson, 1997).

Material behaviour, in the analyses this paper deals with, has been characterized as follows: in uniaxial and biaxial compression by means of second order parabolae, while, in uniaxial tension, as linear-elastic up to the peak, and by means of the exponential softening formula by Hordijk (1991) in the post-peak regime (see Ferrara, 1998 for analytical details). The mechanical parameters which have to be assigned are the compressive and tensile strengths, f_c and f_t , the initial Young modulus and Poisson's ratio, E_0 and ν_0 , the fracture energy G_f and the width of the crack band, w_c , over which localization phenomena are spread out. Starting from the cubic compressive strength experimentally measured by Hassanzadeh (50 MPa), by means of EC2 formulae and with the aid of data available in the literature, the values declared in Fig.1b have been assigned. As can be seen from the graphs in Fig.1c, a reasonable reproduction of the shear behaviour is achieved; the calculated high tails are, in the author's opinion, an almost irrelevant problem, as the more brittle experimental behaviour may be due to unavoidable structural effects owing to the 3D behaviour of the FEN specimen (see below). With reference to normal stress vs. normal displacement curves, it can be seen (Fig.1d) that tensile/compressive transition is captured only for higher values of the δ_s/δ_n ratio and not for $\alpha = 60^\circ, 75^\circ$, where opening mode prevails; by the way, also for lower values of α , the model was not able to reproduce, for the normal stress itself, the reversal in trend after reaching a compressive peak, but an almost indefinite prosecution towards higher and higher compressive values seems to be predicted.

The dilatant character of the model, owing to both the internal variable δ and to the irreversible tensile strain tensor, whose growth is strictly related to damage evolution, makes, for $\alpha = 30^\circ - 45^\circ$, both the principal stresses to become compressive, the principal strains being one tensile and one compressive; consequently it is $\alpha_c = 1$ and $\alpha_t = 0$, according to Eq.(2), and the indirect damage function, which is the slowest one, governs the evolution of the model behaviour being thus responsible of the unrealistic predictions observed before. On the contrary, for $\alpha = 60^\circ - 75^\circ$, applied normal displacement is large enough to allow the first principal stress to remain positive, the second one being slightly compressive (in the order of few MPa); still according to Eq.(2), as ε_{c1}^{el} remains very low, it is $\alpha_c = 0$ and $\alpha_t = 1$, and the model output almost follows uniaxial tension behaviour (for a more detailed explanation see Ferrara, 1998).

In order to make the model well able to reproduce mixed-mode behaviour, without modifying substantially its formulation, which characterizes the model itself as a powerful tool in numerical analyses of concrete behaviour, at least at the specimen-scale level, the author has been decided to act only on the definition of the damage weighting functions in Eq.(2), shifting from an elastic strain approach into a total strain approach, which is also faster and more stable, from a purely computational point of view. The following formulae have been proposed:

$$\alpha_t = H(\text{Tr } \boldsymbol{\varepsilon}) \frac{\text{Tr } \langle \boldsymbol{\varepsilon} \rangle_+}{\text{Tr } |\boldsymbol{\varepsilon}|} \quad - \quad \alpha_c = 1 - \alpha_t \quad (4)$$

$H(\boldsymbol{\varepsilon})$, is the Heaviside step function, here inserted just to set $\alpha_t = 0$ in compressive load-paths. The author is currently working to remove some drawbacks such a formulation

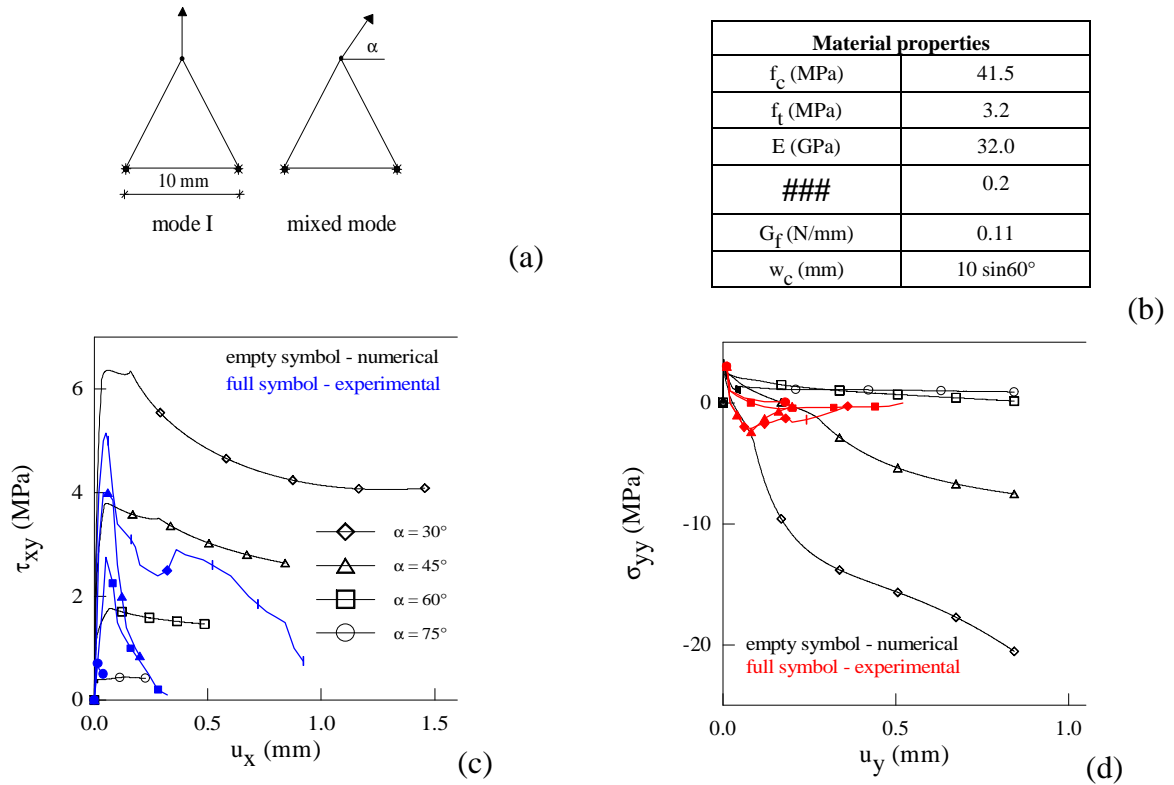
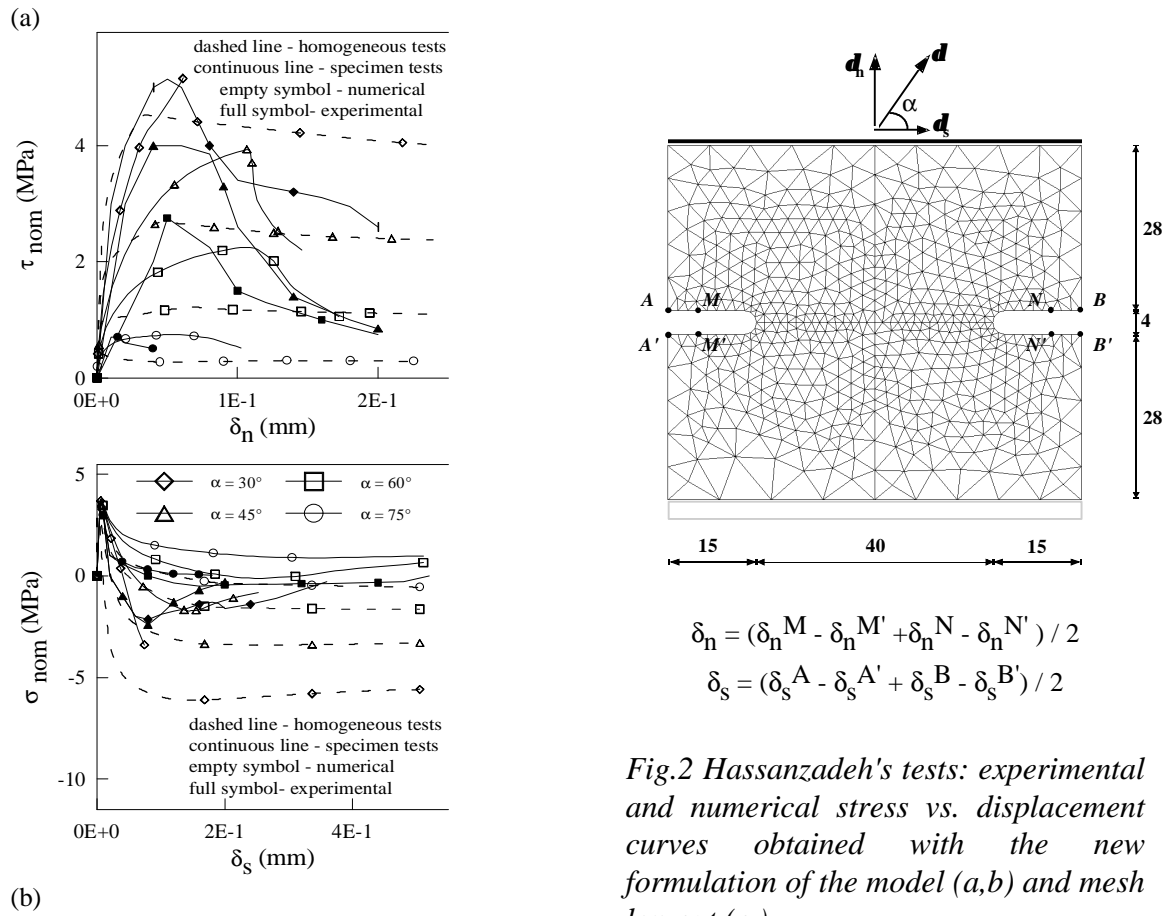


Fig. 1 CST element used for mixed-mode homogeneous tests (a), material parameters (b) and stress vs. displacements curves obtained with original model formulation (c,d)



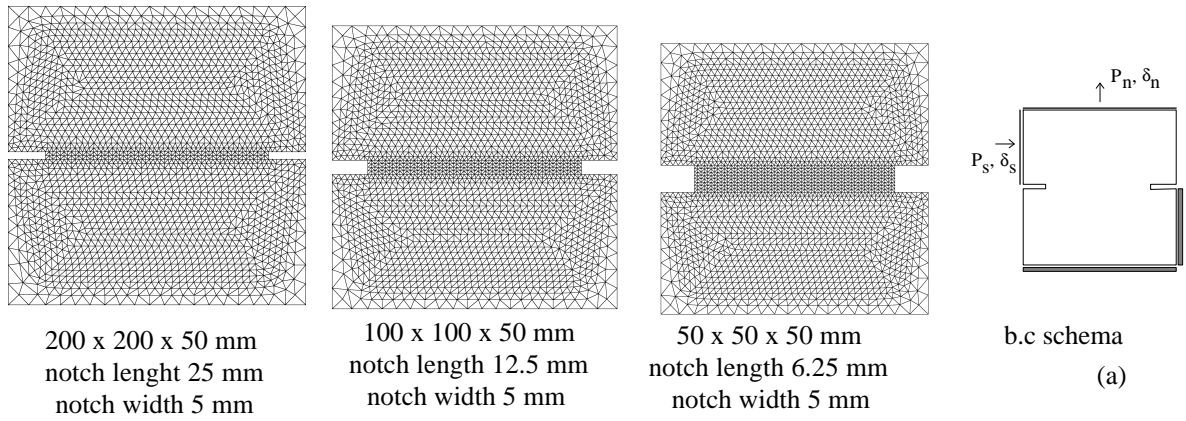
suffers from, in its "rough" version here presented, and which makes it unsuitable for being employed as a general algorithm for calculating damage weighting functions. It has nevertheless been decided to check its reliability in mixed-mode load-paths, starting with the homogeneous tests previously described. The results in Fig.2a-b clearly show as the main target of enhancing model response, in what concerns the normal stress trend, seems to be centered: tensile-compressive transition is correctly reproduced for any value of α and also the reversal in trend after a compressive peak is captured. The more brittle and response recorded in the experiments, may be still attributed to structural effects.

The above said statements about structural 3D effects on the behaviour of the FEN specimen have been checked by simulating the Hassanzadeh's linear paths also at the specimen-scale level. The mesh adopted for such analyses is shown in Fig.2c, with boundary constraints and displacement measurement system also schematically pointed out. Material parameters are the same as quoted in Fig.1b. w_c has been in this case set equal to twice the maximum aggregate size d_a , i.e. to 16 mm, having Hassanzadeh adopted $d_a = 8$ mm; such a choice corresponds to an internal length l equal to $w_c / 8 = 2$ mm (di Prisco and Ferrara, 1996; di Prisco et al., 1998). Computations have been performed in plane strain conditions. It can be seen, still looking at the graphs in Fig.2,a-b, as most of discrepancies between experimental results and model output in homogeneous tests, almost disappear when specimen level computations are performed. By the way, due to the complex geometry of the FEN specimen and to the fact that only its cross section has been simulated in the 2D computations, 3D effects in the growth of fracture process zone and of cracks are lost and neglected. No reliable comparison can be made between numerical and experimental crack patterns as the FEN geometry, though able of inducing an almost homogeneous fracture process zone subjected to mixed-mode loadings, prevented from clear detection of crack growth.

3. SIMULATION OF NOORU-MOHAMMED'S TESTS (PATH 6A)

Let us now pass to examine Nooru-Mohammed's path 6a tests, in which tangential and normal displacements are simultaneously applied to the DEN plate, their ratio being equal to one. A schema of the specimen, with mesh lay-out adopted in the analyses, is shown in Fig. 3a; boundary conditions as well as the dimensions of the investigated specimens are also pointed out. The values of the assigned material parameters are also reported (Fig.3b): they have been calculated, as explained in the preceding paragraph, starting from the experimentally measured compressive and splitting strengths. The crack band width has been determined in agreement with assumptions made in previously performed computations (di Prisco et al., 1998), on the basis of the maximum aggregate diameter (2 mm): for $w_c = 12.6$ mm a value for l equal to 1.6 mm turns out. All the analyses have been performed in plane strain conditions, despite for the larger specimen plane stress ones, whose algorithms are still not available in the employed code (CASTEM2000), would be more realistic.

In Fig. 3,c-d-e computed and experimentally detected crack patterns are compared; a good agreement is achieved, as it can be seen, especially for the largest and for the mean size specimen, though for the latter multiple cracks are spreaded over a quite wider damage band. Also for the smallest plate multiple cracks are smeared over a unique large band, though a "secondary fracture process zone" seems to be captured. Better results could be obtained in the framework of the variable characteristic length approach (di Prisco and Ferrara, 1996), which could allow for taking into account effects of structural gradients on the internal length scale.



Material parameters	
f_c (MPa)	38.5
f_t (MPa)	3
E (GPa) - ν	32 - 0.2
G_f (N/mm)	0.11
w_c (mm)	12.6

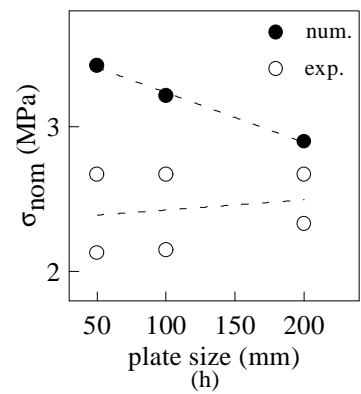
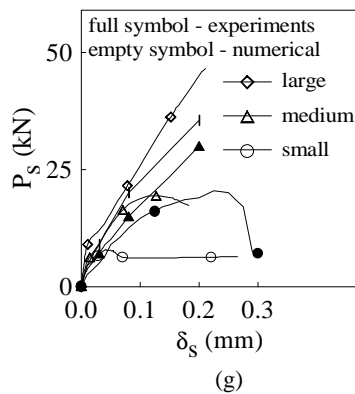
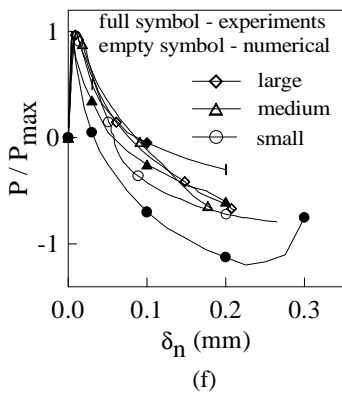
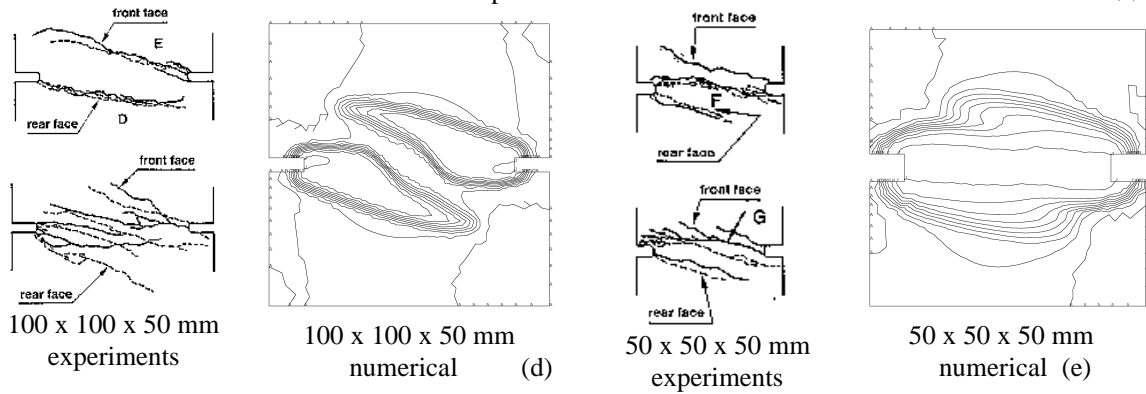
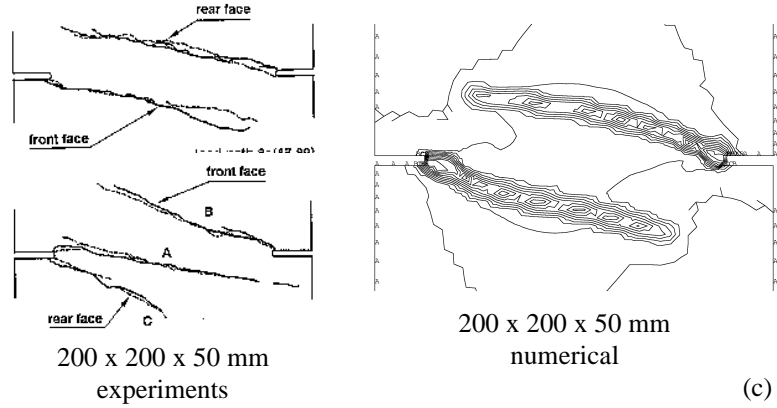


Fig.3 Nooru-Mohammed path6a tests: mesh lay-out for different specimen sizes and boundary conditions schema (a), material parameters (b), experimental and numerical crack patterns (c,d,e), P - d curves (f,g) and size effect on nominal normal strength (h)

Looking at the normal load vs. normal displacement curves (Fig.3f), it can be seen that, while in the experiments a steeper softening has been detected for smaller specimens, with an earlier transition to compressive values, numerical analyses show for the three specimen sizes almost the same behaviour, at least up to the transition point; only further the greater confinement due to the smaller dimensions seems to become active. A gradual transition towards a 3D behaviour, not reproducible in plane strain 2D computations, could partially explain the above detected discrepancies. Nevertheless, in the author's opinion, behaviour of the largest and of the mean-size specimens requires a deeper analysis and further investigations. Taking into account that in the experiments normal displacement have been, for both the above said specimens, measured and controlled over the same length (65 mm), one cannot help thinking that decreasing specimen dimensions seems to have caused an effect similar to increasing measuring length over equally sized specimens. Numerical analyses, in which the same measuring length as in the experiments has been kept and which have furthermore been performed adopting the same characteristic length for all the specimens, provided results which are, in the author's opinion, consistent from a theoretical point of view. Experimental results, on their hand, are likely to confirm structural effects on the "material" length: the notch, whose width is kept constant vs. the specimen size, induces, in smaller specimens, higher and more localized gradients, owing also to the lower degree of heterogeneity of concrete ($d_a = 2$ mm); such gradients may have a lowering effects on the length scale, which now becomes a sort of structural parameter. A greater energy release inside the same length, for the mean size specimen with respect to the largest one, could thus also be a reason for the observed steeper softening. A confirmation of the above said statements could come from size effect on normal strength, "correctly" computed, from a theoretical point of view, and almost absent in the experiments (Fig.3h). Further information could be gathered by investigating, both numerically and experimentally, specimens in which also the notch width is proportionally scaled or testing specimens made by more heterogeneous concrete mixes (greater d_a). Shear curves in Fig. 3g show as, while for the largest plate plane strain conditions always induce confinement with respect to the experiments (an inclined compressive strut working under biaxial compressive conditions is actually modeled!), for smaller plates confinement due to the 3D behaviour of the specimens seems to become, proceeding along the load-path, more and more important, the 2D computations becoming less and less representative. Finally, the higher value for the shear load, computed for the smallest specimen, if compared with results for Hassanzadeh's case $\alpha = 45^\circ$ (10-11 Mpa vs. 4 MPa), rather than to differences in concrete strength, is due to the strongly different boundary conditions, which act on shear transfer mechanisms: while in Hassanzadeh sliding of the upper part of the specimen on the lower one can be supposed to occur, in Nooru-Mohammed horizontal load transfer is demanded to an inclined compressive strut, which furthermore works under out-of-plane confinement due to the 3D behaviour of the specimen. Further information could spring from investigation, both experimental and numerical, on tension/tensile-shear mixed load paths (see also van Mier, 1997), also aiming at a standardization of mixed-mode test methods for concrete.

4. CONCLUSIONS

From the results shown above the following concluding remarks can be drawn:

- the proposed total strain formulation for damage weighting functions enhances the skills of Crush-Crack models at reproducing mixed-mode concrete behaviour. With

respect to the original elastic strain formulation, it is also computationally faster and more stable. Further work has to be done in order to make it mathematically more consistent and suitable for wider applications;

- the influence of structural gradients on the characteristic length seems, once again, to be confirmed. A further investigation with the variable characteristic length approach could be enlightening at the purpose;
- the key role of the boundary conditions in mixed-mode fracture tests, especially in what concerns shear transfer mechanisms and amount, has clearly been outlined. Furthermore, size effects in mixed-mode fracture are still not clearly and completely understood. This makes the need for standard testing in mixed-mode fracture of concrete far from being satisfied.

The investigation on predictive capability of the Crush-Crack model will go on, aiming at modelization of complex shear transfer phenomena occurring in a real r/c structure, such as dowel action mechanism.

5. ACKNOWLEDGEMENTS

The author wishes to express his sincere gratitude to prof. Marco di Prisco for his invaluable scientific and human support, over the entire PhD triennium, and to prof. Pietro Gambarova for his supervision and for having promoted the participation at this Symposium. The financial support of the Italian Ministry for Higher Education and Scientific and Technological Research (MURST) is also gratefully acknowledged.

6. REFERENCES

- Carol, I., Prat, P.C., Lopez, C.M. (1997), "Normal/shear cracking model: application to discrete crack analysis", *ASCE Journal of Engineering Mechanics*, Vol. 123, No.8.
- di Prisco, M., Mazars, J. (1996), "Crush-Crack: a non-local damage model for Concrete", *Mechanics of Cohesive-Frictional Materials*, Vol. 1, pp. 321-347.
- di Prisco, M., Ferrara, L. (1996), "On the progressive localization of fracture processes in concrete", *Studi & Ricerche*, Vol. 17, pp. 1-35
- di Prisco, M., Ferrara, L., Meftah, F., Pamin, J., de Borst, R., Mazars, J., Reynouard, J.M. (1998), "Mixed mode fracture in plain and reinforced concrete: some results on benchmark tests", submitted for publication to *International Journal of Fracture*.
- Ferrara, L. (1998), "Non-local damage approach to mixed mode fracture processes in concrete: a numerical and experimental contribution", *Ph. D. Thesis*, Dept. of Structural Engineering, Politecnico di Milano (in preparation).
- Hassanzadeh, M. (1991), "Behaviour of fracture process zones in concrete influenced by simultaneously applied normal and shear displacements", *Ph. D. Thesis*, Division of Building Materials, Lund Institute of Technology, pp. 1-104.
- Hordijk, D. (1991), "Local approach to fatigue of concrete", *Ph. D. Thesis*, Delft University of Technology, pp. 1-207.
- Nooru-Mohammed, M. B. (1992), "Mixed-mode fracture of concrete: an experimental approach", *Ph. D. Thesis*, Delft University of Technology, pp. 1-149.
- Ohlsson, U., Olofsson, T. (1997), "Mixed-mode fracture and anchor bolts in concrete. Analysis with inner softening bands", *ASCE Journal of Engineering Mechanics*, Vol. 123, No. 10, October, pp. 1027-1033.
- van Mier, J.G.M. (1997), "Fracture processes of concrete", CRC Press, pp. 1-448.